Jussi Salmi, Andreas Richter, and Visa Koivunen. 2006. Enhanced tracking of radio propagation path parameters using state-space modeling. In: Proceedings of the 14th European Signal Processing Conference (EUSIPCO 2006). Florence, Italy. 4-8 September 2006.

ENHANCED TRACKING OF RADIO PROPAGATION PATH PARAMETERS USING STATE-SPACE MODELING

Jussi Salmi, Andreas Richter, Visa Koivunen

Signal Processing Laboratory / SMARAD CoE, Helsinki University of Technology
P.O. Box 3000, FIN-02015 TKK, Finland
phone: + (358) 9 451 2440, fax: + (358) 9 452 3614, email: firstname.lastname@tkk.fi
web: http://wooster.hut.fi

ABSTRACT

Future wireless communication systems will exploit the rich spatial and temporal diversity of the radio propagation environment. This requires new advanced channel models, which need to be verified by real-world channel sounding measurements. In this context the reliable estimation and tracking of the model parameters from measurement data is of particular interest. In this paper, we build a state-space model, and track the propagation parameters with the Extended Kalman Filter in order to capture the dynamics of the channel parameters in time. We then extend the model by considering first order derivatives of the geometrical parameters, which enhances the tracking performance due to improved prediction and robustness against shadowing and fading. The model also includes the effect of distributed diffuse scattering in radio channels. The issue of varying state variable dimension, i.e., the number of propagation paths to track, is also addressed. The performance of the proposed algorithms is demonstrated using both simulated and measured data.

1. INTRODUCTION

The development of radio channel models for wireless MIMO communication systems requires multidimensional channel sounding measurements. The measurements are processed to estimate the radio channel parameters of double-directional channel models [1]. The double-directional modeling allows removal of the influence of the measurement antennas from the observation. This is necessary for using the measurement results for studying and comparing different MIMO transceiver structures. Furthermore, the parameter estimates are required for the statistics of the channel models, and also for validating the employed model.

The extraction of the channel model parameters from the measurement data is done using a parameter estimation algorithm, such as SAGE [2] or RIMAX [3]. A straight-forward approach for estimating the radio channel parameters (such as propagation path delays, angles of arrival and departure, polarized path weight components) is to estimate them for each snapshot independently. However, it can be observed from measurements, that the specular component of the radio channel contains typically propagation paths which persist over a relatively large number of snapshots (time). The parameters of these paths vary slowly in time. This observation can be exploited to track the path parameters over time, in order to reveal dynamic properties of the radio channel. Furthermore, a sequential computation usually reduces complexity of the estimator.

In this paper we use a state-space approach for tracking the radio propagation path parameters over time. This is done by deriving a state-space model based on the nonlinear data model presented in [3], and applying an Extended Kalman Filter (EKF) for parameter estimation. The approach for propagation path parameter estimation using Kalman filtering was introduced in [4]. It was pointed out that the use of a recursive estimation algorithm is computationally less demanding than snapshot-by-snapshot estimation where the time correlation of the parameters is not exploited. One of the drawbacks in [4] is the fact that the state dimension, which is proportional to the number of paths, was kept fixed. This is unrealistic, since paths may appear or disappear in time due to the dynamics in the propagation environment. To overcome this limitation, we propose a hypothesis testing method for state dimension selection. Also the predictor performance of the Kalman filter was limited in [4] due to the simplistic state-space model. We address this problem by extending the state-space model to include first order derivatives of the parameters, which describe the underlying geometry of the propagation paths. This results into improved state prediction, i.e., associating path parameters over time, allowing tracking of the path parameters over some periods of shadowing or crossing of paths.

The paper is structured as follows. In Section 2 we present the observation and the state-space models. In Section 3 we discuss the algorithm and its initialization. In Section 4 we show some estimation results with both artificial, and measurement data. Section 5 concludes this paper.

2. SYSTEM MODEL

The system model of interest can be divided into two parts: the model for a single radio channel observation, and the state-space model describing the evolution from one observation to another. As the observation model we use the double-directional radio channel model [3]. We apply this model to estimate the propagation path parameters: Time Delay of Arrival (TDoA) τ, Direction of Departure (DoD) azimuth φ_T and elevation ϑ_T, Direction of Arrival (DoA) azimuth φ_R and elevation ϑ_R, and four polarimetric path weights γ_{HH}, γ_{HV}, γ_{VH}, and γ_{VV}. The dense multipath component (DMC), describing the stochastic process of distributed diffuse scattering in the radio channel, is also included in the model.

2.1 Model for a Radio Channel Observation

The employed radio channel model consists of two components: the specular (concentrated) propagation component and the dense multipath component, assumed to obey a circular complex Gaussian distribution [3]. In the following, the delay and angular domain parameters (for P paths) are referred to as structural parameters of the model

$$\boldsymbol{\mu} = \left[\boldsymbol{\tau}^{\mathrm{T}}\ \boldsymbol{\varphi}_T^{\mathrm{T}}\ \boldsymbol{\vartheta}_T^{\mathrm{T}}\ \boldsymbol{\varphi}_R^{\mathrm{T}}\ \boldsymbol{\vartheta}_R^{\mathrm{T}}\right]^{\mathrm{T}} \in \mathbb{R}^{5P\times 1}, \tag{1}$$

whereas the path weights for different polarization components (HH = horizontal-to-horizontal, HV = horizontal-to-vertical, etc.)

$$\boldsymbol{\gamma} = \left[\boldsymbol{\gamma}_{HH}^{\mathrm{T}}\ \boldsymbol{\gamma}_{HV}^{\mathrm{T}}\ \boldsymbol{\gamma}_{VH}^{\mathrm{T}}\ \boldsymbol{\gamma}_{VV}^{\mathrm{T}}\right]^{\mathrm{T}} \in \mathbb{C}^{4P\times 1} \tag{2}$$

are referred to as weight parameters. For notational convenience, we have dropped the time index, i.e., $\boldsymbol{\mu} = \boldsymbol{\mu}_k$ (k denotes discrete time), from all the parameters.

The structural parameters $\boldsymbol{\mu} = \left[\boldsymbol{\mu}_1^{\mathrm{T}} \cdots \boldsymbol{\mu}_5^{\mathrm{T}}\right]^{\mathrm{T}}$ are related to the

observation through a complex shift operation [3]

$$\mathbf{A}(\boldsymbol{\mu}_i) = \begin{bmatrix} \mathrm{e}^{-\mathrm{j}(-\frac{N_i-1}{2})\mu_{i,1}} & \dots & \mathrm{e}^{-\mathrm{j}(-\frac{N_i-1}{2})\mu_{i,P}} \\ \vdots & & \vdots \\ \mathrm{e}^{-\mathrm{j}(+\frac{N_i-1}{2})\mu_{i,1}} & \dots & \mathrm{e}^{-\mathrm{j}(+\frac{N_i-1}{2})\mu_{i,P}} \end{bmatrix} \in \mathbb{C}^{N_i \times P}. \tag{3}$$

The shift matrices $\mathbf{A}_i$ are multiplied by the corresponding system responses $\mathbf{G}_i \in \mathbb{C}^{M_i \times N_i}$, yielding

$$\begin{aligned} \mathbf{B}_f &= \mathbf{G}_f \cdot \mathbf{A}(\boldsymbol{\tau}) \\ \mathbf{B}_{R_H} &= \mathbf{G}_{R_H} \cdot (\mathbf{A}(\boldsymbol{\vartheta_R}) \lozenge \mathbf{A}(\boldsymbol{\varphi_R})) \\ \mathbf{B}_{R_V} &= \mathbf{G}_{R_V} \cdot (\mathbf{A}(\boldsymbol{\vartheta_R}) \lozenge \mathbf{A}(\boldsymbol{\varphi_R})) \\ \mathbf{B}_{T_H} &= \mathbf{G}_{T_H} \cdot (\mathbf{A}(\boldsymbol{\vartheta_T}) \lozenge \mathbf{A}(\boldsymbol{\varphi_T})) \\ \mathbf{B}_{T_V} &= \mathbf{G}_{T_V} \cdot (\mathbf{A}(\boldsymbol{\vartheta_T}) \lozenge \mathbf{A}(\boldsymbol{\varphi_T})), \end{aligned}$$

where $\lozenge$ denotes the Khatri-Rao product (column-wise Kronecker-product). Let us introduce the matrix valued function $\mathbf{B}(\boldsymbol{\mu}) \in \mathbb{C}^{M \times 4P}$

$$\begin{aligned} \mathbf{B}(\boldsymbol{\mu}) = [\, & \mathbf{B}_{R_H} \lozenge \mathbf{B}_{T_H} \lozenge \mathbf{B}_f \quad \mathbf{B}_{R_V} \lozenge \mathbf{B}_{T_H} \lozenge \mathbf{B}_f \dots \\ & \mathbf{B}_{R_H} \lozenge \mathbf{B}_{T_V} \lozenge \mathbf{B}_f \quad \mathbf{B}_{R_V} \lozenge \mathbf{B}_{T_V} \lozenge \mathbf{B}_f \,]. \end{aligned} \tag{4}$$

Using (2) and (4), the specular propagation path parameters $\boldsymbol{\mu}$ and $\boldsymbol{\gamma}$ are mapped to an observation vector of length $M = M_f M_T M_R$ with the double-directional channel model as

$$\mathbf{s}(\boldsymbol{\mu}, \boldsymbol{\gamma}) = \mathbf{B}(\boldsymbol{\mu}) \cdot \boldsymbol{\gamma} \in \mathbb{C}^{M \times 1}. \tag{5}$$

The second part of the observation model is comprised of the dense multipath components (DMC) and the measurement noise. The DMC is modeled by a multivariate circular Gaussian process $\mathbf{n}_d \sim \mathcal{N}_c(\mathbf{0}, \mathbf{R}_d) \in \mathbb{C}^{M \times 1}$. The DMC is independent from the measurement noise, which is modeled by a zero-mean circular Gaussian process $\mathbf{n}_m \sim \mathcal{N}_c(\mathbf{0}, \sigma^2 \mathbf{I}) \in \mathbb{C}^{M \times 1}$, σ^2 denoting the noise variance. We combine these random processes $\mathbf{n}_d$ and $\mathbf{n}_m$ into one process yielding

$$\mathbf{n}_y = \mathbf{n}_d + \mathbf{n}_m \sim \mathcal{N}_c(\mathbf{0}, \mathbf{R}_y), \tag{6}$$

with the covariance matrix $\mathbf{R}_y = \mathbf{R}_d + \sigma^2 \mathbf{I}$. The complete model for a radio channel observation is thus approximated as a superposition of P specular propagation paths $\mathbf{s}(\boldsymbol{\mu}, \boldsymbol{\gamma})$ and the random process $\mathbf{n}_y$ as

$$\mathbf{y}_k = \mathbf{s}(\boldsymbol{\mu}_k, \boldsymbol{\gamma}_k) + \mathbf{n}_{y,k}. \tag{7}$$

The vector $\mathbf{y}_k \in \mathbb{C}^{M \times 1}$ represents the output of the channel sounder at time k. The size M of the observation vector depends on the measurement setup. For example TKK's channel sounder [5] aquires $M = M_f M_T M_R = 510 \cdot 32 \cdot 32 = 522240$ complex samples per observation, whereas for the example in this paper we used data from the RUSK sounder [6], having the size $M = M_f M_T M_R = 193 \cdot 16 \cdot 16 = 49408$. Also larger setups for channel sounding exist, and the general trend is towards higher dimensional measurements.

2.2 State-Space Model

We assume that the specular propagation path parameters of the radio channel can be described using a Gauss-Markov model [7]. This allows us to formulate the problem as a state-space model. The state vector $\boldsymbol{\theta}_k \in \mathbb{R}^{PL \times 1}$ contains the structural parameters $\boldsymbol{\mu}_k$, their rate of change $\Delta\boldsymbol{\mu}_k = \frac{d\boldsymbol{\mu}_k}{dt} \cdot \Delta t_k$, and the weight parameters $\boldsymbol{\gamma}_k = \mathbf{a}_k \cdot \mathrm{e}^{\mathrm{j}\boldsymbol{\phi}_k}$. The state vector $\boldsymbol{\theta}_k$ is defined as

$$\begin{aligned} \boldsymbol{\theta}_k = \; & [\, \boldsymbol{\tau}^{\mathrm{T}} \, \Delta\boldsymbol{\tau}^{\mathrm{T}} \, \boldsymbol{\varphi}_T^{\mathrm{T}} \, \Delta\boldsymbol{\varphi}_T^{\mathrm{T}} \, \boldsymbol{\vartheta}_T^{\mathrm{T}} \, \Delta\boldsymbol{\vartheta}_T^{\mathrm{T}} \, \boldsymbol{\varphi}_R^{\mathrm{T}} \, \Delta\boldsymbol{\varphi}_R^{\mathrm{T}} \, \boldsymbol{\vartheta}_R^{\mathrm{T}} \, \Delta\boldsymbol{\vartheta}_R^{\mathrm{T}} \\ & \mathbf{a}_{HH}^{\mathrm{T}} \, \boldsymbol{\phi}_{HH}^{\mathrm{T}} \, \mathbf{a}_{HV}^{\mathrm{T}} \, \boldsymbol{\phi}_{HV}^{\mathrm{T}} \, \mathbf{a}_{VH}^{\mathrm{T}} \, \boldsymbol{\phi}_{VH}^{\mathrm{T}} \, \mathbf{a}_{VV}^{\mathrm{T}} \, \boldsymbol{\phi}_{VV}^{\mathrm{T}} \,]^{\mathrm{T}}, \end{aligned} \tag{8}$$

i.e., the number of parameters in the state is $L = 18$. This choice of parameters enables us to utilize the time dependency of the structural propagation path parameters through the state transition matrix $\boldsymbol{\Phi}$, which is defined, for a single propagation path $P = 1$, as

$$\boldsymbol{\Phi} = \begin{bmatrix} \boldsymbol{\Phi}_\tau & \mathbf{0} & \cdots & \mathbf{0} \\ \mathbf{0} & \boldsymbol{\Phi}_{\varphi_T} & \ddots & \vdots \\ \vdots & \ddots & \ddots & \mathbf{0} \\ \mathbf{0} & \cdots & \mathbf{0} & \boldsymbol{\Phi}_{\gamma_{VV}} \end{bmatrix}, \tag{9}$$

where the sub-matrices for the structural parameters $\boldsymbol{\Phi}_\tau \dots \boldsymbol{\Phi}_{\vartheta_R}$ are defined as

$$\boldsymbol{\Phi}_\mu = \begin{bmatrix} 1 & 1 \\ 0 & 1 \end{bmatrix}, \tag{10}$$

and the sub-matrices $\boldsymbol{\Phi}_{\gamma_{HH}} \dots \boldsymbol{\Phi}_{\gamma_{VV}}$ for the path weight parameters as

$$\boldsymbol{\Phi}_{\gamma_i} = \begin{bmatrix} 1-\nu & 0 \\ 0 & 1 \end{bmatrix}, \tag{11}$$

where a small positive $\nu << 1$ ensures stability. The state transition matrix can be easily extended to several ($P > 1$) propagation paths, a number being in the order of $P = 10 \dots 100$.

With the defined observation model (7), state vector (8), and state transition (9) we can formulate the state-space model as

$$\boldsymbol{\theta}_k = \boldsymbol{\Phi}\boldsymbol{\theta}_{k-1} + \mathbf{v}_k \in \mathbb{R}^{LP \times 1} \tag{12}$$

$$\mathbf{y}_k = \mathbf{s}(\boldsymbol{\theta}_k) + \mathbf{n}_{y,k} \in \mathbb{C}^{M \times 1}, \tag{13}$$

where (12) is the linear state equation and (13) is the nonlinear measurement equation. The state noise $\mathbf{v}_k$ is a real valued white Gaussian process, and it is assumed to be uncorrelated with the state. The covariance matrix $\mathbf{Q}$ of the state noise is a $LP \times LP$ diagonal matrix containing the noise variance of each parameter on the diagonal. The observation noise $\mathbf{n}_{y,k}$ (6) is assumed to be uncorrelated with the state and it has the covariance matrix $\mathbf{R}_{y,k}$.

In [4] the state-space model was based on the Brownian motion model [8], i.e., the motion from snapshot-to-snapshot was modeled only in terms of the Gaussian random state noise process $\mathbf{v}_k$ (the state transition matrix was close to an identity matrix). We improve this model to a constant motion case [8] by including the rate of change of the structural parameters in the state vector (8), and utilize these values in the state transition through (10). The key idea in this more complex motion model is to enhance the tracking of the parameters in dynamic environments by improving prediction. In fact, the order of derivatives included in the state can be further increased for more precise motion modeling. On the other hand, if the motion in the system itself is very small or otherwise limited, then adding any higher order derivatives only increases the computational burden without any gain. Also switching between different levels of model complexity in terms of derivative orders can be implemented as it was suggested for a radar target tracking problem in [9].

For all state-space models, the modeling of the state noise is crucial, because it contains the uncertainty in the model. In the model we propose, the modeling of the state noise process is focused on the uncertainty in the parameters rate of change instead of the actual change. Basically the problem of selecting the most suitable model requires knowledge of the statistics of the underlying process. Since this research work is mainly carried out to collect information about this process the main design goal for the estimator (EKF) is robustness instead of statistical performance.

3. PATH PARAMETER ESTIMATION

The proposed parameter estimation procedure consists of multiple estimators. The core of the algorithm, tracking the propagation path parameters over time, is the EKF. For searching new paths in each

observation a Maximum Likelihood (ML) based (RIMAX [3]) estimator is applied. Also, the parameters of the DMC component, i.e., the covariance matrix $\mathbf{R}_{y,k}$ in (6), are estimated separately. After the EKF and the search for new paths, the reliability of the estimated paths is evaluated. The path estimates that fail our designated threshold test are then dropped from the state. The general principle of the estimation procedure is presented in Figure 1.

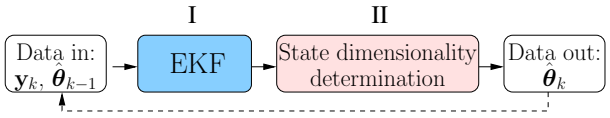

Figure 1: Estimation procedure principle. The state vector $\hat{\boldsymbol{\theta}}_{k-1}$ (as well as other EKF system matrices) of previous time instant may have different dimensions than the current one $\hat{\boldsymbol{\theta}}_k$.

3.1 Extended Kalman Filter

The Extended Kalman Filter uses Taylor series expansion to linearize the nonlinear data model about the current estimates. To apply the EKF one needs to compute the first order partial derivatives to the parameters $\boldsymbol{\theta}$ of the data model $\mathbf{s}(\boldsymbol{\theta})$, i.e., the Jacobian matrix

$$\mathbf{D}(\boldsymbol{\theta}) = \frac{\partial}{\partial \boldsymbol{\theta}^{\mathrm{T}}}\mathbf{s}(\boldsymbol{\theta}) = \left[\frac{\partial}{\partial \theta_1}\mathbf{s}(\boldsymbol{\theta}) \cdots \frac{\partial}{\partial \theta_{LP}}\mathbf{s}(\boldsymbol{\theta})\right]. \quad (14)$$

The expressions for the computation of the EKF can be summarized as [4]:

$$\hat{\boldsymbol{\theta}}_{(k|k-1)} = \boldsymbol{\Phi}\hat{\boldsymbol{\theta}}_{(k-1|k-1)} \quad (15)$$

$$\mathbf{P}_{(k|k-1)} = \boldsymbol{\Phi}\mathbf{P}_{(k-1|k-1)}\boldsymbol{\Phi}^{\mathrm{T}} + \mathbf{Q}_k \quad (16)$$

$$\mathbf{J}(\hat{\boldsymbol{\theta}}_{(k|k-1)}) = 2 \cdot \Re\left\{\mathbf{D}_k^{\mathrm{H}}(\hat{\boldsymbol{\theta}}_{(k|k-1)})\mathbf{R}_{y,k}^{-1}\mathbf{D}_k(\hat{\boldsymbol{\theta}}_{(k|k-1)})\right\}$$

$$\mathbf{P}_{(k|k)} = \left(\mathbf{P}_{(k|k-1)}^{-1} + \mathbf{J}(\hat{\boldsymbol{\theta}}_{(k|k-1)})\right)^{-1} \quad (17)$$

$$\mathbf{q}\left(\mathbf{y}_k|\hat{\boldsymbol{\theta}}_{(k|k-1)}\right) = 2 \cdot \Re\left\{\mathbf{D}_k^{\mathrm{H}}\mathbf{R}_{y,k}^{-1}\left(\mathbf{y}_k - \mathbf{s}\left(\hat{\boldsymbol{\theta}}_{(k|k-1)}\right)\right)\right\}$$

$$\Delta\hat{\boldsymbol{\theta}}_k = \mathbf{P}_{(k|k-1)}\left(\mathbf{I} - \mathbf{J}(\hat{\boldsymbol{\theta}}_{(k|k-1)})\mathbf{P}_{(k|k)}\right) \cdot \mathbf{q}\left(\mathbf{y}_k|\hat{\boldsymbol{\theta}}_{(k|k-1)}\right) \quad (18)$$

$$\hat{\boldsymbol{\theta}}_{(k|k)} = \hat{\boldsymbol{\theta}}_{(k|k-1)} + \Delta\hat{\boldsymbol{\theta}}_k, \quad (19)$$

where

$$\mathbf{q}\left(\mathbf{y}_k|\boldsymbol{\theta}, \mathbf{R}_{y,k}\right) = \frac{\partial}{\partial \boldsymbol{\theta}}\mathcal{L}(\mathbf{y}|\boldsymbol{\theta}, \mathbf{R}_{y,k})$$

is the score function, i.e., the partial derivative of the log-likelihood function with respect to the parameters $\boldsymbol{\theta}$, and

$$\mathbf{J}(\boldsymbol{\theta}, \mathbf{R}_{y,k}) = -\mathrm{E}\left\{\frac{\partial}{\partial \boldsymbol{\theta}}\mathcal{L}(\mathbf{y}_k|\boldsymbol{\theta}, \mathbf{R}_{y,k})\left(\frac{\partial}{\partial \boldsymbol{\theta}}\mathcal{L}(\mathbf{y}_k|\boldsymbol{\theta}, \mathbf{R}_{y,k})\right)^{\mathrm{T}}\right\}$$

is the Fisher information matrix [10].

3.2 State Dimension Determination

Due to the dynamical nature of the radio propagation environments, the number of estimated paths, i.e., the state dimension, varies in time. We determine the state dimensionality, i.e., the number of paths to be tracked, through a two stage procedure:

1. A search procedure for new paths, and
2. a dropping criteria for unreliable paths.

The search for new paths is relying on the Maximum Likelihood estimation based RIMAX algorithm [3]. It is performed at each observation after the EKF filtering stage by providing the number of paths to search, and the residual $\mathbf{y}_k - \mathbf{s}(\hat{\boldsymbol{\theta}}_{(k|k)})$ as the input for RIMAX. The RIMAX algorithm evaluates the reliability of the new paths resulting in $0 - P_{new}$ estimates, which are added to the state.

Dropping of unreliable paths from the state is based on the Wald test [11]. We select the estimated path weight amplitudes of each path p as our test parameters $\boldsymbol{\theta}_r = \mathbf{a}_p = \left[a_{HH,p} \cdots a_{VV,p}\right]^{\mathrm{T}}$. The test hypotheses for each path p are $\mathbb{H}_0 : \boldsymbol{\theta}_r = \mathbf{0}$ and $\mathbb{H}_1 : \boldsymbol{\theta}_r \neq \mathbf{0}$. Path p is valid (hypothesis $\mathbb{H}_1$ holds) if

$$T_W = \hat{\boldsymbol{\theta}}_r^{\mathrm{T}}\left([\mathbf{P}_{k|k}]_{\theta_r\theta_r}\right)^{-1}\hat{\boldsymbol{\theta}}_r > \epsilon, \quad (20)$$

where $[\mathbf{P}]_{\theta_r\theta_r} \in \mathbb{R}^{N_r \times N_r}$ is a matrix containing the columns and rows related to the parameters $\boldsymbol{\theta}_r$. T_W is χ^2 distributed with degrees of freedom ($df = N_r$). Thus ϵ is defined as

$$\Pr(x > \epsilon) = 1 - \int_0^{\epsilon} \chi_{df}^2(x)dx = c_\epsilon, \quad (21)$$

and its value can be chosen to correspond to a confidence level c_ϵ of the probability of hypothesis $\mathbb{H}_0$ given T_W.

A detailed description of the implemented algorithm is shown in Figure 2.

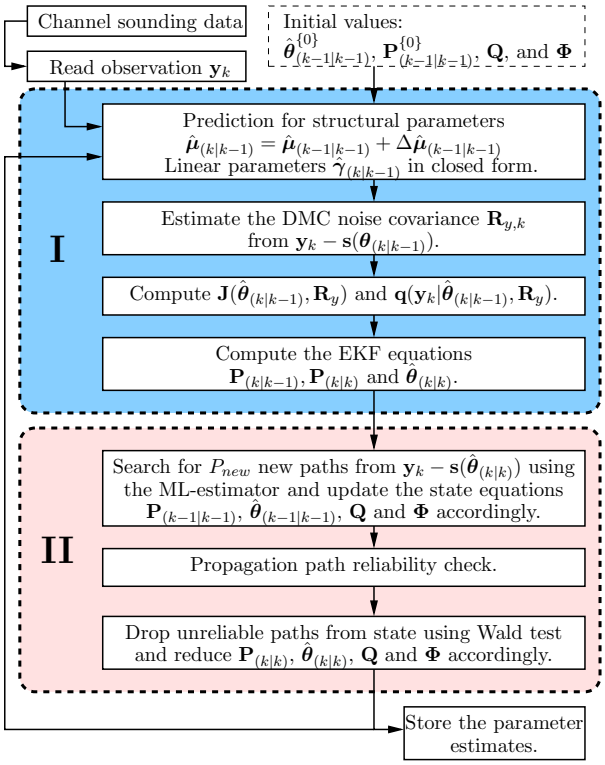

Figure 2: Complete estimation procedure. The upper level concepts in Figure 1 are marked with areas I and II.

4. ESTIMATION EXAMPLES

4.1 Estimator performance in simulations

To justify the usage of the proposed motion model we compared the performance of two state-space motion models: one with the rate of change included only as uncertainty in the state noise covariance, and the other one having the first order derivatives of the parameters with respect to time in the state. Two sets of noisy artificial data were generated for simulations. The first set of data is for a static propagation path, i.e., the parameters remain constant over time. The second simulation was run for data generated for a

single propagation path in an environment with a moving receiver and a moving scatterer. In this situation the motion of the objects is linear, whereas the rate of change of the parameters is nonlinear. The deviation of the delays and directions of arrival from the linear state-space model depends on the distance of the two passing objects.

The simulation was run for 100 realizations, i.e., observations were generated using the same parameter values, but independent noise realizations. We used the instantaneous RMS error of the estimates as the performance criterion. The RMS error is defined as

$$\sigma_\mu = \sqrt{\frac{1}{R}\sum_{r=1}^{R}(\mu_r - \hat{\mu}_r)^2}, \tag{22}$$

where R is the number of realizations.

The results for RMS estimation error of the static scenario are shown in Figure 3. Figure 3(a) shows the RMS estimation error in

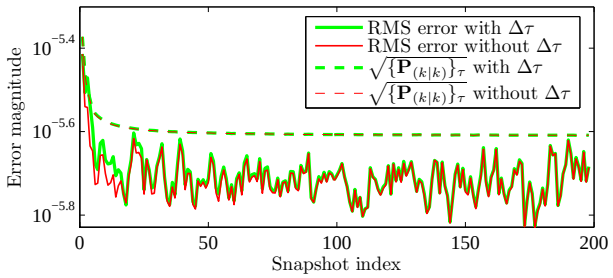

(a) RMS estimation error for normalized delay.

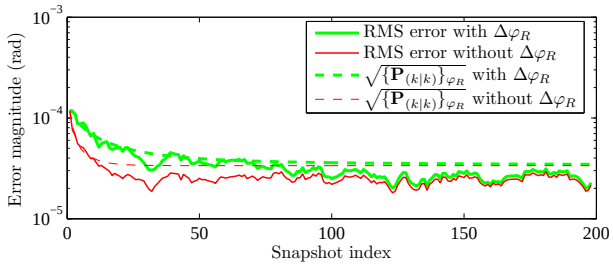

(b) RMS estimation error for Rx azimuth.

Figure 3: Comparison of RMS estimation errors of two state-space motion models. Simulation was run for 100 realizations over 200 snapshots for a static propagation path. The two approaches have practically the same performance.

normalized delay over time, and Figure 3(b) represents the error in Rx azimuth. The dashed lines in the figures represent the estimated error standard deviation, given by the square root of the corresponding diagonal value of the filtering error covariance matrix $\mathbf{P}_{(k|k)}$ (17). From the results in Figure 3 we can conclude that in the case of estimating static propagation paths, the enhanced motion model does not improve the performance in terms of RMS estimation error.

The simulation was run for dynamic data with a propagation path under constant motion. Figure 4(a) shows the RMS error comparison for the normalized delay, and Figure 4(b) illustrates the estimation error for azimuth AoA. From Figure 4 it can be observed that for tracking the propagation path parameters, which are changing due to linear motion, the improved motion model clearly outperforms the simpler one.

4.2 Performance using measured data

The performance of the estimator was validated in practice using real world measurement data. The measurement campaign was

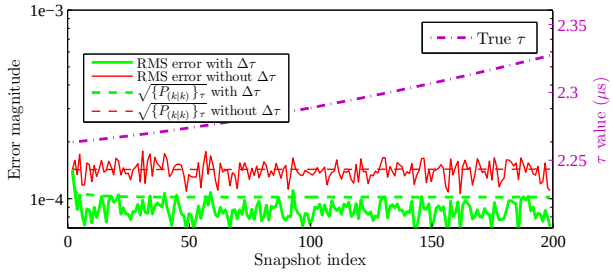

(a) RMS estimation error for normalized delay.

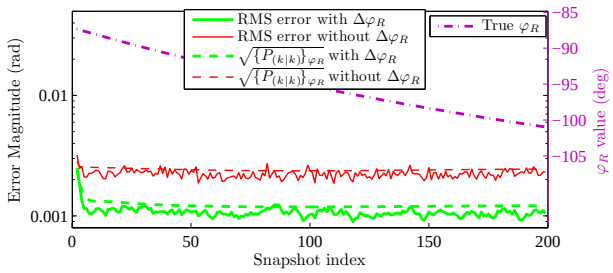

(b) RMS estimation error for Tx azimuth.

Figure 4: Comparison of RMS estimation errors of two state-space motion models. Simulation was run for 100 realizations over 200 snapshots for a dynamic propagation path in constant motion. The value of the estimated parameters are shown by the dash-dotted lines. Improved motion model results in lower error variance.

conducted by Institute of Communications and Measurement Engineering, Ilmenau University of Technology and Medav GmbH on August 12th 2004 at Ilmenau city center using the RUSK channel sounder [6]. The transmit (Tx) antenna array was a 16 element UCA (Uniform Circular Array) placed on a measurement trolley. The receive (Rx) array was an 8 element dual polarized ULA (Uniform Linear Array). This setup enables the estimation of the parameters in (8), excluding the elevation at the receiver (ϑ_R) due to elevation ambiguity of the ULA. Also half of the polarization components (γ_{HH} and γ_{HV}) are not used due to single polarized Tx array. For a detailed description of the measurement, see [6].

The estimation results visualized here are for a route of the Tx coming from a non-line-of-sight street canyon to a line-of-sight open square where the Rx is located. Figure 5 shows the comparison of the Power Delay Profile (PDP) of the measurement, and the reconstruction from EKF estimates. The PDPs are averaged over all channels (Tx-Rx antenna pairs). Figure 6 shows the comparison of

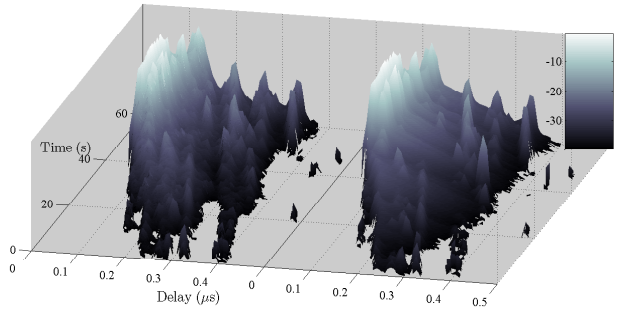

Figure 5: Comparison of measured (left) and EKF reconstructed (right) power delay profiles. The EKF reconstruction includes also the effect of the DMC estimate, which can be observed as an exponentially decaying slope below the peaks resulting from the strongest path estimates.

the Tx azimuth angle estimates of the same measurement. The EKF estimates have a good match with the estimates from a maximum

likelihood based RIMAX [3] estimator. It can also be observed that the EKF tracks some of the propagation paths for a longer time than RIMAX. Currently the EKF is dropping the path estimates if they are shadowed, but the improved prediction makes it possible to track the paths also during a limited period of shadowing or fading.

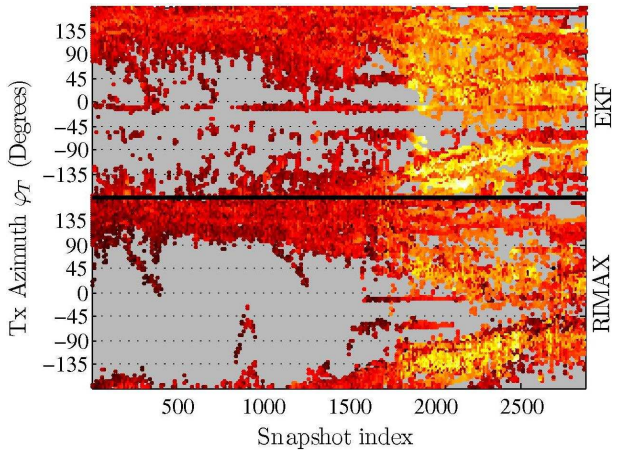

Figure 6: DoD azimuth angle estimates processed from measurement data. Lighter color denotes stronger paths. The EKF is tracking some of the paths for a longer time.

The parameter estimation of radio channel sounding measurements consumes traditionally a huge amount of computation time. One of the most noticeable practical improvements of the EKF compared to, e.g., RIMAX, is the significantly reduced complexity. Due to the recursive nature of the EKF, the filter itself is computationally much less demanding compared to the iterative maximum likelihood (Levenberg-Marquardt) used in RIMAX. Figure 7(a) shows the time required for processing each snapshot for this particular measurement route. The EKF has about one order of magnitude lower complexity than RIMAX, although the number of estimated paths (see Figure 7(b)) is about the same.

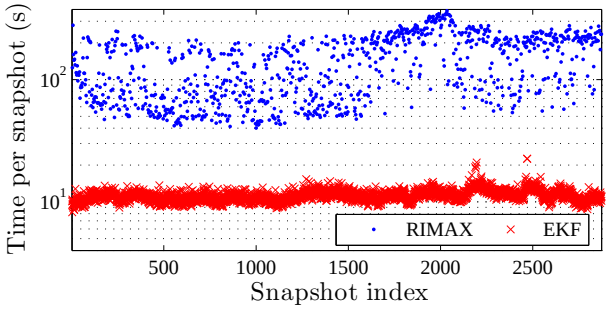

(a) Processing time of EKF vs. RIMAX.

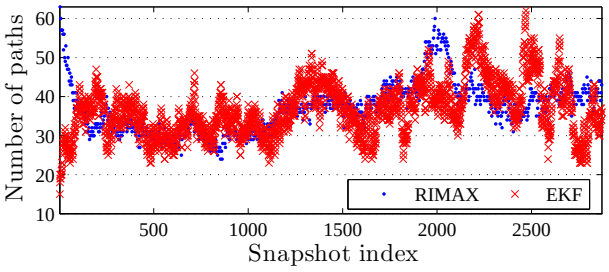

(b) Number of estimated paths EKF vs. RIMAX.

Figure 7: Comparison of estimation time and estimated number of paths for EKF implementation vs. RIMAX.

5. CONCLUSIONS

In this paper we introduce an enhanced state-space model for tracking the radio channel propagation path parameters. This improved model includes the rate of change of the structural parameters in the state vector allowing enhanced prediction and path association from snapshot to snapshot. Reliable prediction can also enable tracking of paths over short term fading. Our simulations confirm that, in the case of (close to) linear motion in the measurement environment, the estimator using the improved state space model outperforms the one where motion is not taken into account. We also address the selection of the model order, i.e., the number of propagation paths to track. Estimation results from channel sounding measurements show that the proposed method produces promising results with significantly reduced computational complexity compared to, e.g., the RIMAX algorithm.

6. ACKNOWLEDGEMENTS

The authors would like to thank Institute of Communications and Measurement Engineering of Ilmenau University of Technology and Medav GmbH for providing the RUSK channel sounder measurement data.

REFERENCES

[1] M. Steinbauer, A. Molisch, and E. Bonek, "The double-directional radio channel," *IEEE Antennas and Propagation Magazine*, vol. 43, no. 4, pp. 51–63, Aug. 2001.

[2] B. H. Fleury, M. Tschudin, R. Heddergott, D. Dahlhaus, and K. I. Pedersen, "Channel parameter estimation in mobile radio environments using the SAGE algorithm," *IEEE J. Select. Areas Commun.*, vol. 17, no. 3, pp. 434–450, Mar. 1999.

[3] A. Richter, "Estimation of radio channel parameters: Models and algorithms," Ph. D. dissertation, Technische Universität Ilmenau, Germany, 2005, ISBN 3-938843-02-0, urn:nbn:de:gbv:ilm1-2005000111. [Online]. Available: www.db-thueringen.de

[4] A. Richter, M. Enescu, and V. Koivunen, "State-space approach to propagation path parameter estimation and tracking," in *Proc. 6th IEEE Workshop on Signal Processing Advances in Wireless Communications*, New York City, June 2005.

[5] V.-M. Kolmonen, J. Kivinen, L. Vuokko, and P. Vainikainen, "5.3 GHz MIMO radio channel sounder," in *Proc. 22nd Instrumentation and Measurement Technology Conference, IMTC'05*, Ottawa, Ontario, Canada, May 16-19 2005, pp. 1883–1888.

[6] U. Trautwein, M. Landmann, G. Sommerkorn, and R. Thomä, "System-Oriented Measurement and Analysis of MIMO Channels," *COST273 12th Management Committee Meeting*, Jan 19-21, 2005, Bologna, Italy, TD(05)063.

[7] J. M. Mendel, *Lessons in Estimation Theory for Signal Processing, Communications, and Control*. Englewood Cliffs, NJ: Prentice-Hall, Inc., 1995.

[8] L. D. Stone, C. A. Barlow, and T. L. Corwin, *Bayesian Multiple Target Tracking*. Norwood, MA: Artech House Inc., 1999.

[9] B. Slocumb, P. West, T. Shirey, and E. Kamen, "Tracking a maneuvering target in the presence of false returns and ECM using a variable state dimension Kalman filter," in *Proc. of American Control Conference*, vol. 4, Seattle, WA, USA, June 1995, pp. 2611–2615.

[10] L. Scharf, *Statistical Signal Processing, Detection Estimation and Time Series Analysis*. Reading, MA: Addison-Wesley, 1990.

[11] S. M. Kay, *Fundamentals of Statistical Signal Processing: Detection Theory*. Prentice-Hall International, 1998, vol. 2.